

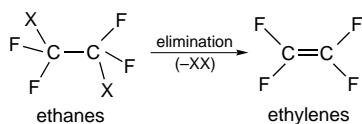
Femtosecond Elimination Reaction Dynamics

D. Zhong, S. Ahmad, and A. H. Zewail*

Arthur Amos Noyes Laboratory of Chemical Physics
California Institute of Technology
Pasadena, California 91125

Received March 31, 1997

In this paper, we report our femtosecond (fs) clocking of an elimination reaction with multi-bond breakage:



The elimination involves the (α , β) two C–X bonds ($X = \text{I}$) and leads to the transformation of ethanes to ethylenes, a general class of halogen-atom elimination (and addition) in many organic reactions.¹ By measurements of (1) the fs time evolution of products, (2) the product–velocity distributions, and (3) the recoil anisotropy (at 277 nm), the reaction dynamics and mechanism are microscopically elucidated: the two-center elimination is a two-step, *nonconcerted* process with the reaction involving the intermediate $\text{C}_2\text{F}_4\text{I}^\ddagger$. The time scales for the two bond fissions are two orders of magnitude different: the *primary* bond breakage only takes about 200 fs, but the *secondary* elimination needs 25 ps. The former is due to the repulsive force in the C–I bond caused by the promotion of the HOMO n electron to the LUMO σ^* orbital, while for the latter elimination is directly governed by the energy redistribution and the rate of bond breakage of $\text{C}_2\text{F}_4\text{I}^\ddagger$.

The reaction was studied in a supersonic molecular beam integrated with the femtosecond apparatus.² The velocity distributions of iodine products were obtained using the approach of kinetic-energy resolved, time-of-flight (KETOF) mass spectrometry with resonance-enhanced multiphoton ionization (centered at 304 nm, for both I and I^* with about equal efficiency) detection. The recoil anisotropy was determined by using polarized femtosecond pulses, as detailed elsewhere.²

A typical TOF mass spectrum is shown in Figure 1. With the femtosecond resolution, we clearly see the parent mass peak. The I^+ KETOF distributions for the parallel ($\chi = 0^\circ$) and magic angle ($\chi = 54.7^\circ$) excitation are also displayed for 1 ps vs 600 ps reaction times. For the magic angle KETOF shape at 1 ps, the velocity distribution is essentially flat, as predicted by theory for a direct femtosecond dissociation.² Indeed, this distribution reflects the primary C–I bond breakage. At longer times, however, the distribution displays a buildup of intensity around $V_z \approx 0$, shown at 600 ps, reflecting the process of the secondary C–I elimination. A similar conclusion is reached for the $\chi = 0^\circ$ results. To obtain the complete temporal behavior, we gated the slow velocity portion of the distribution ($-250 \leq V_z \leq 250$ m/s) at the magic angle while varying the time delay. The biexponential rise of the femtosecond transient (Figure 2) gives the two distinct reaction times for the two steps of C–I elimination: $\tau_1 \approx 200$ fs and $\tau_2 = 25$ ps, consistent with the behavior of the KETOF distributions.

From the magic angle I^+ KETOF distribution, we obtained² the laboratory recoil *speed* distribution of I atoms at 1 ps reaction time (Figure 2). Two distributions peaked at 850 and 1200 m/s were obtained for the primary elimination which correspond to the formation of the product in both spin–orbit states, I^* and I, a characteristic of alkyl halide³ bond breakage with femtosecond

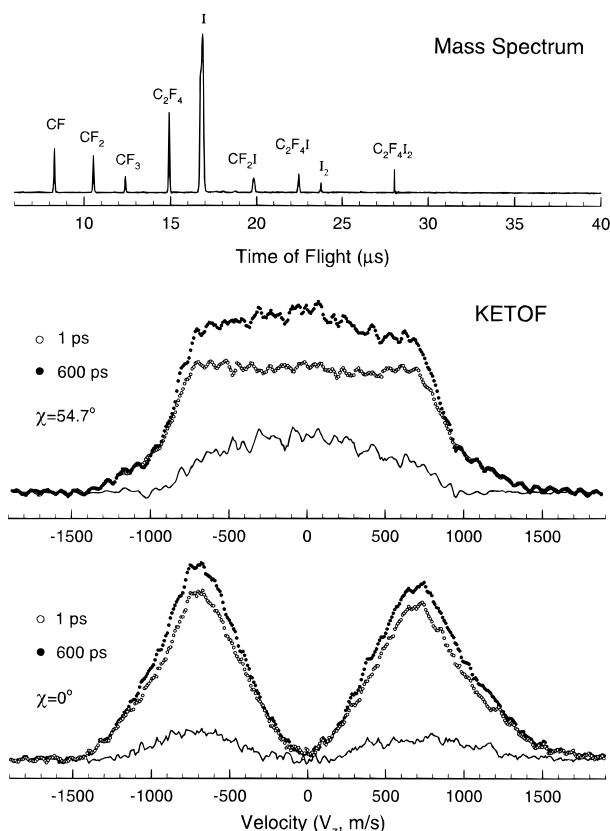


Figure 1. TOF mass spectrum (top) from expansions of $\text{C}_2\text{F}_4\text{I}_2$ vapor at -35°C and 700 Torr of He (monomer condition). The I^+ KETOF distributions are also shown for two typical delay times of 1 and 600 ps. The χ is the angle of the linear femtosecond laser polarization relative to the TOF axis (z). The difference of each two KETOF distributions (solid line) represents the contribution of the secondary bond cleavage.

dissociation times.⁴ This large translational energy release in such short time excludes the possibility of breaking two C–I bonds concertedly. The excitation energy is 103 kcal/mol, and if two bonds ($\Delta H \approx 59$ kcal/mol for the I channel)⁵ are involved, no such translational energy can be produced. This conclusion is entirely consistent with the biexponential transient behavior in Figure 2; the first “rise” (~ 200 fs) is due to the primary elimination. (For methyl iodide, this process actually takes 150 fs.⁴) From measurements of the polarization dependence of the I^+ KETOF distribution (parallel vs magic angle), we also deduced the anisotropy parameter: $2.0 \leq \beta \leq 1.9$. The value is close to an ideal parallel transition ($\beta = 2.0$) (*i.e.*, the transition moment is parallel to the C–I bond direction) and again is consistent with the observed prompt elimination process caused by the pure repulsive force.

In the primary C–I breakage, we observe that the I^* and I branching is 0.7 and 0.3, respectively. This branching is similar to that observed in CH_3I .^{3,4,6} If all available energy is converted to translational motion, the expected speeds are indicated by the arrows in Figure 2, and the observed distributions do indeed reach these maximum values (1100 m/s for I^* and 1460 m/s for I). The average translational energy release, $\langle E_T \rangle / E_{\text{avl}}$, for

(3) See: Riley, S. J.; Wilson, K. R. *Faraday Discuss. Chem. Soc.* **1972**, 53, 132.

(4) Zhong, D.; Cheng, P. Y.; Zewail, A. H. *J. Chem. Phys.* **1996**, 105, 7864.

(5) Nathanson, G. M.; Minton, T. K.; Shane, S. F.; Lee, Y. T. *J. Chem. Phys.* **1989**, 90, 6157.

(6) For example, see: Godwin, F. G.; Paterson, C.; Gorry, P. A. *Mol. Phys.* **1987**, 61, 827. Hess, W. P.; Kohler, S. J.; Haugen, H. K.; Leone, S. R. *J. Chem. Phys.* **1986**, 84, 2143. Sparks, R. K.; Shobatake, K.; Carlson, L. R.; Lee, Y. T. *J. Chem. Phys.* **1981**, 75, 3838.

(1) Lowry, T. H.; Richardson, K. S. *Mechanism and Theory in Organic Chemistry*, 3rd ed.; Harper & Row: New York, 1987.

(2) Zewail, A. H. *Femtochemistry: Ultrafast Dynamics of the Chemical Bond, Vol. I and II*; World Scientific: Singapore, 1994. Cheng, P. Y.; Zhong, D.; Zewail, A. H. *J. Chem. Phys.* **1996**, 105, 6216.

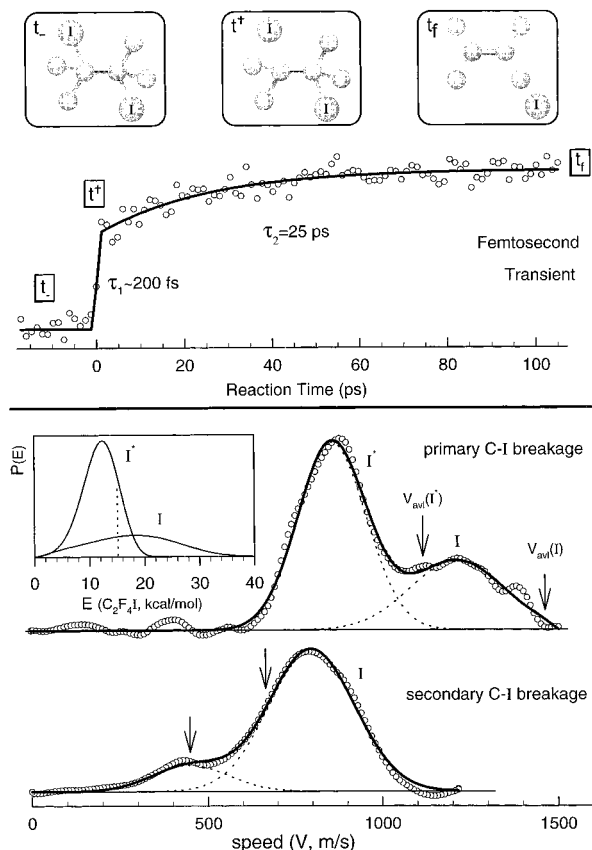


Figure 2. The experimental femtosecond transient (top), together with a biexponential theoretical fit (solid line). Three structures are shown to indicate the reaction: prior to the femtosecond excitation (t_-), after the primary bond breakage (t^+), and when the final elimination (t_f) is reached. The recoil speed distributions from the primary and secondary C–I bond breakage, deduced (and smoothed) from the magic angle data in Figure 1, are shown in the bottom half; the solid lines are Gaussian fits of the observed distributions. The two arrows in the secondary speed distribution indicate the peak speeds of the dissociating C_2F_4I radicals produced from the I^* and I channels (see the text). The internal energy distributions of the C_2F_4I radical after the primary elimination are shown in the insert. The dashed line shows the deduced decomposition threshold of C_2F_4I into C_2F_4 and I .

each channel is found to be 59% for I^* and 67% for I . Both translational energy distributions are broad, and the full-width at half-maximum is 8.5 kcal/mol for I^* and 19.5 kcal/mol for I . Theoretically, we predict that 86% of the available energy should appear as translation for a rigid radical (no vibrational excitation) following an impulsive bond breakage; for a “soft” radical, we obtained 13%.⁷ Our experimental values are more toward the rigid radical limit.

The secondary elimination dynamics have different reaction times and velocity characteristic, but surprisingly similar recoil anisotropy. After the femtosecond primary elimination, the observed 25 ps rise of the I atom (Figure 2) represents the time scale for the redistribution to deposit enough energy in the reaction coordinate of the intermediate $[CF_2I-CF_2]^+$ to break the second C–I bond. This is consistent with the previous picosecond studies⁸ and is further supported by the observation of the broad speed distribution of I atoms from the secondary elimination (Figure 2).

The velocity distribution for I atoms from the secondary bond breakage ($\chi = 0^\circ$ of Figure 1) shows a very high angular anisotropy, and the deduced anisotropy parameter (β) is ~ 1.9 , nearly the same as that for the primary bond breakage. Since the rotational time of the C_2F_4I intermediate is estimated to be

between 2 and 8 ps, shorter than the observed 25 ps reaction time, the secondary elimination produces an isotropic, small speed distribution of I atoms. The addition of this small velocity to the large velocity (see below) of the center-of-mass velocity of the C_2F_4I radical does not destroy the initial ($t = 0$) alignment (*i.e.*, the anisotropy of the secondary process “remembers” the primary elimination anisotropy and is determined mainly by the larger center-of-mass velocity of C_2F_4I). Thus, even though the measured anisotropy is very high, it does not reflect the long-lived state of the intermediate and would have erroneously predicted a short-lived intermediate.

The internal energy distribution of the C_2F_4I intermediate can be obtained from conservation of energy and is shown in the insert of Figure 2. This distribution is broad with two peaks at 12 and 17 kcal/mol for the primary I^* and I channels. Comparing the I atom yield (Figure 1, $\chi = 54.7^\circ$) from the secondary elimination with the total primary iodine product, only $\sim 30\%$ of the intermediate dissociates into C_2F_4 and I . From $P(E)$ vs E in the insert, we therefore deduce an activation energy of ~ 15 kcal/mol;⁹ the area under the distribution of E greater than 15 kcal/mol is about 30%. This indicates that a small portion of C_2F_4I dissociates when it is created from the I^* channel, while a large fraction decomposes if the I channel is involved; the secondary elimination produces ground state I atoms⁸ because of the energetics. The weakness of the second C–I bond is due to a concerted path that breaks the C–I bond while forming a new C=C π bond,¹⁰ in contrast with the primary elimination which involves C–I cleavage. Preliminary RRKM calculations of the radical dissociation rate give the picosecond time scale. However, it is not clear that the secondary elimination is akin to complete thermal behavior, as discussed below.

Considering the decomposition threshold of ~ 15 kcal/mol (see the insert in Figure 2), the dissociating C_2F_4I radicals resulting from the primary I^* and I channels have two peak speeds at 450 and 670 m/s (arrows in Figure 2, bottom), respectively. The recoil speed distribution of the secondary I atoms shows two peaks at ~ 450 and ~ 800 m/s. These peak values of the radical and the secondary I atom for the I^* channel are the same. This equality supports the previous description of the secondary elimination process. However, the values for the I channel differ by 130 m/s (800 vs 670 m/s). In addition to the expected ~ 670 m/s peak distribution for the secondary I atoms, it appears that a higher speed component (~ 800 m/s) is part of the distribution which reflects a faster dissociation of the intermediate with higher internal energies, possibly in a nonthermal distribution.

In conclusion, with femtosecond-resolved mass spectrometry, we are able to study in real time the elementary dynamics of two-center elimination processes and to resolve the *state*, *velocity*, and *angular* evolution of products. The reaction is highly nonconcerted and involves an intermediate with a barrier determined by the concerted breakage of a $\sigma(C-I)$ bond and the making of a π bond. The intermediate is formed in 200 fs at the initial structure after the detachment⁴ of one atom, and dynamical entry of the transition state is critical to any nonstatistical behavior. Molecular dynamics should be of interest to elucidate reaction trajectories.¹¹

Acknowledgment. This work was supported by a grant from the National Science Foundation.

JA9710013

(9) An activation energy of 7.1 ± 2.5 kcal/mol has been reported.⁵ The difference may be due to the difficulty in separating the I^* and I channels at 308 nm excitation (very broad distributions).⁵ Note that stimulated dissociation of the intermediate is, in our case, negligible as we do not observe the 470 m/s peak at 1 ps.

(10) The weak C–I bond energy in the C_2F_4I radical can be estimated from $D_0(C-I) - D_0(C=C) = \sim 8$ kcal/mol. With this ΔH value and the fact that I addition to $C=C$ is endothermic, our value of the effective barrier (potential + centrifugal) is consistent with being larger than ~ 8 kcal/mol. For discussion of the C=C double bond energy, see: Carter, E. A.; Goddard, W. A. *J. Am. Chem. Soc.* **1988**, *110*, 4077.

(11) Polanyi, J. C. *Acc. Chem. Res.* **1972**, *5*, 161.

(7) Busch, G. E.; Wilson, K. R. *J. Chem. Phys.* **1972**, *56*, 3626, 3638.
 (8) Knee, J. L.; Khundkar, L. R.; Zewail, A. H. *J. Chem. Phys.* **1985**, *83*, 1996. Khundkar, L. R.; Zewail, A. H. *Ibid.* **1990**, *92*, 231.